nature

SUPPLEMENTARY INFORMATION

https://doi.org/10.1038/s41586-019-1196-1

In the format provided by the authors and unedited.

Cavity quantum electrodynamics with atom-like mirrors

Mohammad Mirhosseini[1,2,3,8], Eunjong Kim[1,2,3,8], Xueyue Zhang[1,2,3], Alp Sipahigil[1,2,3], Paul B. Dieterle[1,2,3], Andrew J. Keller[1,2,3], Ana Asenjo-Garcia[3,4,5,6], Darrick E. Chang[5,7] & Oskar Painter[1,2,3]*

[1]Kavli Nanoscience Institute, California Institute of Technology, Pasadena, CA, USA. [2]Thomas J. Watson, Sr., Laboratory of Applied Physics, California Institute of Technology, Pasadena, CA, USA. [3]Institute for Quantum Information and Matter, California Institute of Technology, Pasadena, CA, USA. [4]Norman Bridge Laboratory of Physics, California Institute of Technology, Pasadena, CA, USA. [5]ICFO-Institut de Ciencies Fotoniques, The Barcelona Institute of Science and Technology, Barcelona, Spain. [6]Physics Department, Columbia University, New York, NY, USA. [7]ICREA-Institució Catalana de Recerca i Estudis Avançats, Barcelona, Spain. [8]These authors contributed equally: Mohammad Mirhosseini, Eunjong Kim. *e-mail: opainter@caltech.edu

I. SUPPLEMENTARY NOTE 1: SPECTROSCOPIC MEASUREMENT OF INDIVIDUAL QUBITS

The master equation of a qubit in a thermal bath at temperature T, driven by a classical field is given by $\dot{\hat{\rho}} = -i[\hat{H}/\hbar, \hat{\rho}] + \mathcal{L}[\hat{\rho}]$, where the Hamiltonian $\hat{H}$ and the Liouvillian $\mathcal{L}$ is written as [1]

$$\hat{H}/\hbar = -\frac{\omega_\mathrm{p} - \omega_\mathrm{q}}{2}\,\hat{\sigma}_z + \frac{\Omega_\mathrm{p}}{2}\,\hat{\sigma}_x, \tag{S-1}$$

$$\mathcal{L}[\hat{\rho}] = (\bar{n}_\mathrm{th}+1)\Gamma_1\mathcal{D}[\hat{\sigma}_-]\hat{\rho} + \bar{n}_\mathrm{th}\Gamma_1\mathcal{D}[\hat{\sigma}_+]\hat{\rho} + \frac{\Gamma_\varphi}{2}\mathcal{D}[\hat{\sigma}_z]\hat{\rho}. \tag{S-2}$$

Here, ω_p (ω_q) is the frequency of the drive (qubit), Ω_p is the Rabi frequency of the drive, $\bar{n}_\mathrm{th} = 1/(e^{\hbar\omega_\mathrm{q}/k_\mathrm{B}T} - 1)$ is the thermal occupation of photons in the bath, Γ_1 and Γ_φ are relaxation rate and pure dephasing rates of the qubit, respectively. The superoperator

$$\mathcal{D}[\hat{A}]\hat{\rho} = \hat{A}\hat{\rho}\hat{A}^\dagger - \frac{1}{2}\{\hat{A}^\dagger\hat{A}, \hat{\rho}\} \tag{S-3}$$

denotes the Lindblad dissipator. The master equation can be rewritten in terms of density matrix elements $\rho_{a,b} \equiv \langle a|\hat{\rho}|b\rangle$ as

$$\dot{\rho}_\mathrm{e,e} = \frac{i\Omega_\mathrm{p}}{2}(\rho_\mathrm{e,g} - \rho_\mathrm{g,e}) - (\bar{n}_\mathrm{th}+1)\Gamma_1\rho_\mathrm{e,e} + \bar{n}_\mathrm{th}\Gamma_1\rho_\mathrm{g,g} \tag{S-4}$$

$$\dot{\rho}_\mathrm{e,g} = \left[i(\omega_\mathrm{p} - \omega_\mathrm{q}) - \frac{(2\bar{n}_\mathrm{th}+1)\Gamma_1 + 2\Gamma_\varphi}{2}\right]\rho_\mathrm{e,g} + \frac{i\Omega_\mathrm{p}}{2}(\rho_\mathrm{e,e} - \rho_\mathrm{g,g}) \tag{S-5}$$

$$\dot{\rho}_\mathrm{g,e} = \dot{\rho}^*_\mathrm{e,g}; \quad \dot{\rho}_\mathrm{g,g} = -\dot{\rho}_\mathrm{e,e} \tag{S-6}$$

With $\rho_\mathrm{e,e} + \rho_\mathrm{g,g} = 1$, the steady-state solution ($\dot{\hat{\rho}} = 0$) to the master equation can be expressed as

$$\rho^\mathrm{ss}_\mathrm{e,e} = \frac{\bar{n}_\mathrm{th}}{2\bar{n}_\mathrm{th}+1}\frac{1 + (\delta\omega/\Gamma_2^\mathrm{th})^2}{1 + (\delta\omega/\Gamma_2^\mathrm{th})^2 + \Omega_\mathrm{p}^2/(\Gamma_1^\mathrm{th}\Gamma_2^\mathrm{th})} + \frac{1}{2}\frac{\Omega_\mathrm{p}^2/(\Gamma_1^\mathrm{th}\Gamma_2^\mathrm{th})}{1 + (\delta\omega/\Gamma_2^\mathrm{th})^2 + \Omega_\mathrm{p}^2/(\Gamma_1^\mathrm{th}\Gamma_2^\mathrm{th})}, \tag{S-7}$$

$$\rho^\mathrm{ss}_\mathrm{e,g} = -i\frac{\Omega_\mathrm{p}}{2\Gamma_2^\mathrm{th}(2\bar{n}_\mathrm{th}+1)}\frac{1 + i\,\delta\omega/\Gamma_2^\mathrm{th}}{1 + (\delta\omega/\Gamma_2^\mathrm{th})^2 + \Omega_\mathrm{p}^2/(\Gamma_1^\mathrm{th}\Gamma_2^\mathrm{th})}, \tag{S-8}$$

where $\delta\omega = \omega_\mathrm{p} - \omega_\mathrm{q}$ is the detuning of the drive from qubit frequency, $\Gamma_1^\mathrm{th} = (2\bar{n}_\mathrm{th}+1)\Gamma_1$ and $\Gamma_2^\mathrm{th} = \Gamma_1^\mathrm{th}/2 + \Gamma_\varphi$ are the thermally enhanced decay rate and dephasing rate of the qubit.

Now, let us consider the case where a qubit is coupled to the waveguide with decay rate of Γ_1D. If we send in a probe field $\hat{a}_\mathrm{in}$ from left to right along the waveguide, the right-propagating output field $\hat{a}_\mathrm{out}$ after interaction with the qubit is written as [2]

$$\hat{a}_\mathrm{out} = \hat{a}_\mathrm{in} + \sqrt{\frac{\Gamma_\mathrm{1D}}{2}}\hat{\sigma}_-.$$

The probe field creates a classical drive on the qubit with the rate of $\Omega_\mathrm{p}/2 = -i\langle\hat{a}_\mathrm{in}\rangle\sqrt{\Gamma_\mathrm{1D}/2}$. With the steady-state solution of master equation (S-8) the transmission amplitude $t = \langle\hat{a}_\mathrm{out}\rangle/\langle\hat{a}_\mathrm{in}\rangle$ can be written as

$$t(\delta\omega) = 1 - \frac{\Gamma_\mathrm{1D}}{2\Gamma_2^\mathrm{th}(2\bar{n}_\mathrm{th}+1)}\frac{1 + i\,\delta\omega/\Gamma_2^\mathrm{th}}{1 + (\delta\omega/\Gamma_2^\mathrm{th})^2 + \Omega_\mathrm{p}^2/(\Gamma_1^\mathrm{th}\Gamma_2^\mathrm{th})}. \tag{S-9}$$

At zero temperature ($\bar{n}_\mathrm{th} = 0$) Eq. (S-9) reduces to [3, 4]

$$t(\delta\omega) = 1 - \frac{\Gamma_\mathrm{1D}}{2\Gamma_2}\frac{1 + i\,\delta\omega/\Gamma_2}{1 + (\delta\omega/\Gamma_2)^2 + \Omega_\mathrm{p}^2/(\Gamma_1\Gamma_2)}. \tag{S-10}$$

Here, $\Gamma_2 = \Gamma_\varphi + \Gamma_1/2$ is the dephasing rate of the qubit in the absence of thermal occupancy. In the following, we define the parasitic decoherence rate of the qubit as $\Gamma' = 2\Gamma_2 - \Gamma_\mathrm{1D} = \Gamma_\mathrm{loss} + 2\Gamma_\varphi$, where Γ_loss denotes the decay rate of qubit induced by channels other than the waveguide. Examples of Γ_loss in superconducting qubits include dielectric loss, decay into slotline mode, and loss from coupling to two-level system (TLS) defects.

A. Effect of saturation

To discuss the effect of saturation on the extinction in transmission, we start with the zero temperature case of Eq. (S-10). We introduce the saturation parameter $s \equiv \Omega_{\rm p}^2/\Gamma_1\Gamma_2$ to rewrite the on-resonance transmittivity as

$$t(0) = 1 - \frac{\Gamma_{1\rm D}}{2\Gamma_2}\frac{1}{1+s} \approx 1 - \frac{\Gamma_{1\rm D}}{2\Gamma_2}(1-s) = \left(1 + s\frac{\Gamma_{1\rm D}}{\Gamma'}\right)\left(\frac{\Gamma'}{\Gamma' + \Gamma_{1\rm D}}\right), \tag{S-11}$$

where the low-power assumption $s \ll 1$ has been made in the last step. For the extinction to get negligible effect from saturation, the power-dependent part in Eq. (S-11) should be small compared to the power-independent part. This is equivalent to $s < \Gamma'/\Gamma_{1\rm D}$. Using the relation

$$\Omega_{\rm p} = \sqrt{\frac{2\Gamma_{1\rm D}P_{\rm p}}{\hbar\omega_{\rm q}}}$$

between the driven Rabi frequency and the power $P_{\rm p}$ of the probe and assuming $\Gamma' \ll \Gamma_{1\rm D}$, this reduces to

$$P_{\rm p} \lesssim \frac{\hbar\omega_{\rm q}\Gamma'}{4}. \tag{S-12}$$

In the experiment, the probe power used to resolve the extinction was -150 dBm (10^{-18} W), which gives a limit to the observable Γ' due to our coherent drive of $\Gamma'/2\pi \approx 150$ kHz.

B. Effect of thermal occupation

To take into account the effect of thermal occupancy, we take the limit where the saturation is very small ($\Omega_{\rm p} \approx 0$). On resonance, the transmission amplitude is expressed as

$$t(0) = 1 - \frac{\Gamma_{1\rm D}}{[(2\bar{n}_{\rm th}+1)\Gamma_1 + 2\Gamma_\varphi](2\bar{n}_{\rm th}+1)} \approx 1 - \frac{\Gamma_{1\rm D}}{2\Gamma_2} + \frac{(\Gamma_1+\Gamma_\varphi)\Gamma_{1\rm D}}{\Gamma_2^2}\bar{n}_{\rm th}, \tag{S-13}$$

where we have assumed the thermal occupation is very small, $\bar{n}_{\rm th} \ll 1$. In the limit where $\Gamma_{1\rm D}$ is dominating spurious loss and pure dephasing rates ($\Gamma_2 \approx \Gamma_{1\rm D}/2$), this reduces to

$$t(0) \approx t(0)|_{T=0} + 4\bar{n}_{\rm th} \tag{S-14}$$

and hence the thermal contribution dominates the transmission amplitude unless $\bar{n}_{\rm th} < \Gamma'/4\Gamma_{1\rm D}$.

Using this relation, we can estimate the upper bound on the temperature of the environment based on our measurement of extinction. We have measured the transmittance of Q_1 at its maximum frequency (Figure S-1) before and after installing a thin-film microwave attenuator, which is customized for proper thermalization of the input signals sent into the waveguide with the mixing chamber plate of the dilution refrigerator [5]. The minimum transmittance was measured to be $|t|^2 \approx 1.7 \times 10^{-4}$ (2.1×10^{-5}) before (after) installation of the attenuator, corresponding to the upper bound on thermal photon number of $\bar{n}_{\rm th} \lesssim 3.3 \times 10^{-3}$ (1.1×10^{-3}). With the attenuator, this corresponds to temperature of 43 mK, close to the temperature values reported in Ref. [5].

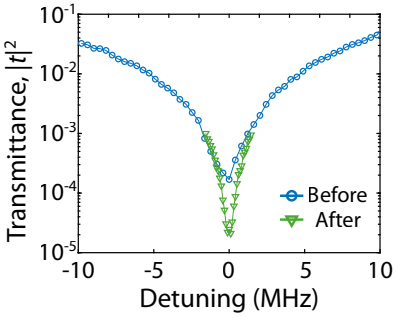

FIG. S-1. **Effect of thermal occupancy on extinction.** The transmittance of Q_1 is measured at the flux-insensitive point before and after installation of customized microwave attenuator. We observe an order-of-magnitude enhancement in extinction after the installation, indicating a better thermalization of input signals to the chip.

II. SUPPLEMENTARY NOTE 2: DETAILED MODELING OF THE ATOMIC CAVITY

In this section, we analyze the atomic cavity discussed in the main text in more detail, taking into account its higher excitation levels. The atomic cavity is formed by two identical *mirror* qubits [frequency $\omega_{\rm q}$, decay rate $\Gamma_{\rm 1D}$ (Γ') to waveguide (spurious loss) channel placed at $\lambda/2$ distance along the waveguide (Figure 1a). From the $\lambda/2$ spacing, the correlated decay of the two qubits is maximized to $-\Gamma_{\rm 1D}$, while the exchange interaction is zero. This results in formation of dark state $|{\rm D}\rangle$ and bright state $|{\rm B}\rangle$

$$|{\rm D}\rangle = \frac{|{\rm eg}\rangle + |{\rm ge}\rangle}{\sqrt{2}}, \quad |{\rm B}\rangle = \frac{|{\rm eg}\rangle - |{\rm ge}\rangle}{\sqrt{2}}, \tag{S-15}$$

which are single-excitation states of two qubits with suppressed and enhanced waveguide decay rates $\Gamma_{\rm 1D,D} = 0$, $\Gamma_{\rm 1D,B} = 2\Gamma_{\rm 1D}$ to the waveguide. Here, g (e) denotes the ground (excited) state of each qubit. Other than the ground state $|{\rm G}\rangle \equiv |{\rm gg}\rangle$, there also exists a second excited state $|{\rm E}\rangle \equiv |{\rm ee}\rangle$ of two qubits, completing $2^2 = 4$ eigenstates in the Hilbert space of two qubits. We can alternatively define $|{\rm D}\rangle$ and $|{\rm B}\rangle$ in terms of collective annihilation operators

$$\hat{S}_{\rm D} = \frac{1}{\sqrt{2}}\left(\hat{\sigma}_-^{(1)} + \hat{\sigma}_-^{(2)}\right), \quad \hat{S}_{\rm B} = \frac{1}{\sqrt{2}}\left(\hat{\sigma}_-^{(1)} - \hat{\sigma}_-^{(2)}\right) \tag{S-16}$$

as $|{\rm D}\rangle = \hat{S}_{\rm D}^\dagger|{\rm G}\rangle$ and $|{\rm B}\rangle = \hat{S}_{\rm B}^\dagger|{\rm G}\rangle$. Here, $\hat{\sigma}_-^{(i)}$ de-excites the state of i-th mirror qubit. Note that the doubly-excited state $|{\rm E}\rangle$ can be obtained by successive application of either $\hat{S}_{\rm D}^\dagger$ or $\hat{S}_{\rm B}^\dagger$ twice on the ground state $|{\rm G}\rangle$.

The interaction of qubits with the field in the waveguide is written in the form of $\hat{H}_{\rm WG} \propto (\hat{S}_{\rm B} + \hat{S}_{\rm B}^\dagger)$, and hence the state transfer via classical drive on the waveguide can be achieved only between states of non-vanishing transition dipole $\langle f|\hat{S}_{\rm B}|i\rangle$. In the present case, only $|{\rm G}\rangle \leftrightarrow |{\rm B}\rangle$ and $|{\rm B}\rangle \leftrightarrow |{\rm E}\rangle$ transitions are available via the waveguide with the same transition dipole. This implies that the waveguide decay rate of $|{\rm E}\rangle$ is equal to that of $|{\rm B}\rangle$, $\Gamma_{\rm 1D,E} = 2\Gamma_{\rm 1D}$.

To investigate the level structure of the dark state, which is not accessible via the waveguide channel, we introduce an ancilla *probe* qubit [frequency $\omega_{\rm q}$, decay rate $\Gamma_{\rm 1D,p}$ ($\Gamma'_{\rm p}$) to waveguide (loss) channel] at the center of mirror qubits. The probe qubit is separated by $\lambda/4$ from mirror qubits, maximizing the exchange interaction to $\sqrt{\Gamma_{\rm 1D,p}\Gamma_{\rm 1D}}/2$ with zero correlated decay. This creates an interaction of excited state of probe qubit to the dark state of mirror qubits $|{\rm e}\rangle_{\rm p}|{\rm G}\rangle \leftrightarrow |{\rm g}\rangle_{\rm p}|{\rm D}\rangle$, while the bright state remains decoupled from this dynamics.

The master equation of the three-qubit system reads $\dot{\hat{\rho}} = -i[\hat{H}/\hbar, \hat{\rho}] + \mathcal{L}[\hat{\rho}]$, where the Hamiltonian $\hat{H}$ and the Liouvillian $\mathcal{L}$ are given by

$$\hat{H} = \hbar J\left[\hat{\sigma}_-^{\rm (p)}\hat{S}_{\rm D}^\dagger + \hat{\sigma}_+^{\rm (p)}\hat{S}_{\rm D}\right] \tag{S-17}$$

$$\mathcal{L}[\hat{\rho}] = (\Gamma_{\rm 1D,p} + \Gamma'_{\rm p})\,\mathcal{D}\left[\hat{\sigma}_-^{\rm (p)}\right]\hat{\rho} + (2\Gamma_{\rm 1D} + \Gamma')\,\mathcal{D}\left[\hat{S}_{\rm B}\right]\hat{\rho} + \Gamma'\,\mathcal{D}\left[\hat{S}_{\rm D}\right]\hat{\rho} \tag{S-18}$$

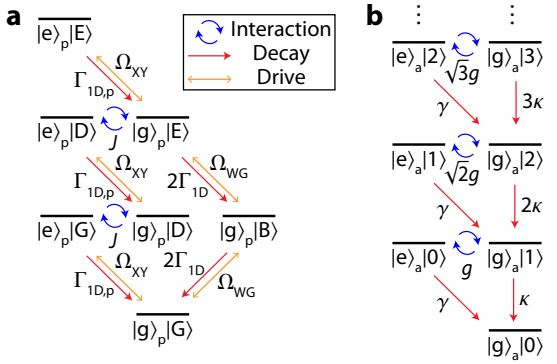

FIG. S-2. **Level structure of the atomic cavity and linear cavity.** a. Level structure of the three-qubit system of probe qubit and atomic cavity. $\Gamma_{\rm 1D,p}$ and $2\Gamma_{\rm 1D}$ denotes the decay rates into the waveguide channel, $\Omega_{\rm XY}$ is the local drive on the probe qubit, and $\Omega_{\rm WG}$ is the drive from the waveguide. The coupling strength J is the same for the first excitation and second excitation levels, b. Level structure of an atom coupled to a linear cavity. $|e\rangle_{\rm a}$ ($|g\rangle_{\rm a}$) denotes the excited state (ground state) of the atom, while $|n\rangle$ is the n-photon Fock state of the cavity field. g is the coupling, γ is the decay rate of the atom, and κ is the photon loss rate of the cavity.

Here, $\hat{\sigma}_{\pm}^{(\mathrm{p})}$ are the Pauli operators for the probe qubit, $2J = \sqrt{2\Gamma_{1\mathrm{D,p}}\Gamma_{1\mathrm{D}}}$ is the interaction between probe qubit and dark state, and $\mathcal{D}[\cdot]$ is the Lindblad dissipator defined in Eq. (S-3). The full level structure of the $2^3 = 8$ states of three qubits and the rates in the system are summarized in Fig. S-2a. Note that the effective (non-Hermitian) Hamiltonian $\hat{H}_{\mathrm{eff}}$ in the main text can be obtained from absorbing part of the Liouvillian in Eq. (S-18) excluding terms associated with quantum jumps.

To reach the dark state of the atomic cavity, we first apply a local gate $|\mathrm{g}\rangle_{\mathrm{p}}|\mathrm{G}\rangle \to |\mathrm{e}\rangle_{\mathrm{p}}|\mathrm{G}\rangle$ on the probe qubit (Ω_{XY} in Fig. S-2a) to prepare the state in the first-excitation manifold. Then, the Rabi oscillation $|\mathrm{e}\rangle_{\mathrm{p}}|\mathrm{G}\rangle \leftrightarrow |\mathrm{g}\rangle_{\mathrm{p}}|\mathrm{D}\rangle$ takes place with the rate of J. We can identify $g = J$, $\gamma = \Gamma_{1\mathrm{D,p}} + \Gamma'_{\mathrm{p}}$, $\kappa = \Gamma'$ in analogy to cavity QED (Fig. 1a and Fig. S-2b) and calculate cooperativity as

$$\mathcal{C} = \frac{(2J)^2}{\Gamma_{1,\mathrm{p}}\Gamma_{1,\mathrm{D}}} = \frac{2\Gamma_{1\mathrm{D,p}}\Gamma_{1\mathrm{D}}}{(\Gamma_{1\mathrm{D,p}} + \Gamma'_{\mathrm{p}})\Gamma'} \approx \frac{2\Gamma_{1\mathrm{D}}}{\Gamma'},$$

when the spurious loss rate Γ' is small. A high cooperativity can be achieved in this case due to collective suppression of radiation in atomic cavity and cooperative enhancement in the interaction, scaling linearly with the Purcell factor $P_{1\mathrm{D}} = \Gamma_{1\mathrm{D}}/\Gamma'$. Thus, we can successfully map the population from the excited state of probe qubit to dark state of mirror qubits with the interaction time of $(2J/\pi)^{-1}$.

Going further, we attempt to reach the second-excited state $|\mathrm{E}\rangle = (\hat{S}_{\mathrm{D}}^{\dagger})^2|\mathrm{G}\rangle$ of atomic cavity. After the state preparation of $|\mathrm{g}\rangle_{\mathrm{p}}|\mathrm{D}\rangle$ mentioned above, we apply another local gate $|\mathrm{g}\rangle_{\mathrm{p}}|\mathrm{D}\rangle \to |\mathrm{e}\rangle_{\mathrm{p}}|\mathrm{D}\rangle$ on the probe qubit and prepare the state in the second-excitation manifold. In this case, the second excited states $|\mathrm{e}\rangle_{\mathrm{p}}|\mathrm{D}\rangle \leftrightarrow |\mathrm{g}\rangle_{\mathrm{p}}|\mathrm{E}\rangle$ have interaction strength J, same as the first excitation, while the $|\mathrm{E}\rangle$ state becomes highly radiative to waveguide channel. The cooperativity $\mathcal{C}$ is calculated as

$$\mathcal{C} = \frac{(2J)^2}{\Gamma_{1,\mathrm{p}}\Gamma_{1,\mathrm{E}}} = \frac{2\Gamma_{1\mathrm{D,p}}\Gamma_{1\mathrm{D}}}{(\Gamma_{1\mathrm{D,p}} + \Gamma'_{\mathrm{p}})(2\Gamma_{1\mathrm{D}} + \Gamma')} < 1,$$

which is always smaller than unity. Therefore, the state $|\mathrm{g}\rangle_{\mathrm{p}}|\mathrm{E}\rangle$ is only virtually populated and the interaction maps the population in $|\mathrm{e}\rangle_{\mathrm{p}}|\mathrm{D}\rangle$ to $|\mathrm{g}\rangle_{\mathrm{p}}|\mathrm{B}\rangle$ with the rate of $(2J)^2/(2\Gamma_{1\mathrm{D}}) = \Gamma_{1\mathrm{D,p}}$. This process competes with radiative decay (at a rate of $\Gamma_{1\mathrm{D,p}}$) of probe qubit $|\mathrm{e}\rangle_{\mathrm{p}}|\mathrm{D}\rangle \to |\mathrm{g}\rangle_{\mathrm{p}}|\mathrm{D}\rangle$ followed by the Rabi oscillation in the first-excitation manifold, giving rise to damped Rabi oscillation in Fig. 3f.

A. Effect of phase length mismatch

Deviation of phase length between mirror qubits from $\lambda/2$ along the waveguide can act as a non-ideal contribution in the dynamics of atomic cavity. The waveguide decay rate of dark state can be written as $\Gamma_{1\mathrm{D,D}} = \Gamma_{1\mathrm{D}}(1 - |\cos\phi|)$, where $\phi = k_{1\mathrm{D}}d$ is the phase separation between mirror qubits [2]. Here, $k_{1\mathrm{D}}$ is the wavenumber and d is the distance between mirror qubits.

We consider the case where the phase mismatch $\Delta\phi = \phi - \pi$ of mirror qubits is small. The decay rate of the dark state scales as $\Gamma_{1\mathrm{D,D}} \approx \Gamma_{1\mathrm{D}}(\Delta\phi)^2/2$ only adding a small contribution to the decay rate of dark state. Based on the decay rate of dark states from time-domain measurement in Table S-2, we estimate the upper bound on the phase mismatch $\Delta\phi/\pi$ to be 5% for type-I and 3.5% for type-II.

B. Effect of asymmetry in $\Gamma_{1\mathrm{D}}$

So far we have assumed that the waveguide decay rate $\Gamma_{1\mathrm{D}}$ of mirror qubits are identical and neglected the asymmetry. If the waveguide decay rates of mirror qubits are given by $\Gamma_{1\mathrm{D},1} \neq \Gamma_{1\mathrm{D},2}$, the dark state and bright state are redefined as

$$|\mathrm{D}\rangle = \frac{\sqrt{\Gamma_{1\mathrm{D},2}}|\mathrm{eg}\rangle + \sqrt{\Gamma_{1\mathrm{D},1}}|\mathrm{ge}\rangle}{\sqrt{\Gamma_{1\mathrm{D},1} + \Gamma_{1\mathrm{D},2}}}, \quad |\mathrm{B}\rangle = \frac{\sqrt{\Gamma_{1\mathrm{D},1}}|\mathrm{eg}\rangle - \sqrt{\Gamma_{1\mathrm{D},2}}|\mathrm{ge}\rangle}{\sqrt{\Gamma_{1\mathrm{D},1} + \Gamma_{1\mathrm{D},2}}}, \tag{S-19}$$

with collectively suppressed and enhanced waveguide decay rates of $\Gamma_{1\mathrm{D,D}} = 0$, $\Gamma_{1\mathrm{D,B}} = \Gamma_{1\mathrm{D},1} + \Gamma_{1\mathrm{D},2}$, remaining fully dark and fully bright even in the presence of asymmetry. We also generalize Eq. (S-16) as

$$\hat{S}_{\mathrm{D}} = \frac{\sqrt{\Gamma_{1\mathrm{D},2}}\hat{\sigma}_{-}^{(1)} + \sqrt{\Gamma_{1\mathrm{D},1}}\hat{\sigma}_{-}^{(2)}}{\sqrt{\Gamma_{1\mathrm{D},1} + \Gamma_{1\mathrm{D},2}}}, \quad \hat{S}_{\mathrm{B}} = \frac{\sqrt{\Gamma_{1\mathrm{D},1}}\hat{\sigma}_{-}^{(1)} - \sqrt{\Gamma_{1\mathrm{D},2}}\hat{\sigma}_{-}^{(2)}}{\sqrt{\Gamma_{1\mathrm{D},1} + \Gamma_{1\mathrm{D},2}}}. \tag{S-20}$$

With this basis, the Hamiltonian can be written as

$$\hat{H} = \hbar J_{\mathrm{D}} \left(\hat{\sigma}_{-}^{(\mathrm{p})} \hat{S}_{\mathrm{D}}^{\dagger} + \hat{\sigma}_{+}^{(\mathrm{p})} \hat{S}_{\mathrm{D}} \right) + \hbar J_{\mathrm{B}} \left(\hat{\sigma}_{-}^{(\mathrm{p})} \hat{S}_{\mathrm{B}}^{\dagger} + \hat{\sigma}_{+}^{(\mathrm{p})} \hat{S}_{\mathrm{B}} \right), \tag{S-21}$$

where

$$J_{\mathrm{D}} = \frac{\sqrt{\Gamma_{1\mathrm{D,p}}\Gamma_{1\mathrm{D},1}\Gamma_{1\mathrm{D},2}}}{\sqrt{\Gamma_{1\mathrm{D},1}+\Gamma_{1\mathrm{D},2}}}, \quad J_{\mathrm{B}} = \frac{\sqrt{\Gamma_{1\mathrm{D,p}}}(\Gamma_{1\mathrm{D},1}-\Gamma_{1\mathrm{D},2})}{2\sqrt{\Gamma_{1\mathrm{D},1}+\Gamma_{1\mathrm{D},2}}}.$$

Thus, the probe qubit interacts with both the dark state and bright state with the ratio of $J_{\mathrm{D}} : J_{\mathrm{B}} = 2\sqrt{\Gamma_{1\mathrm{D},1}\Gamma_{1\mathrm{D},2}} : (\Gamma_{1\mathrm{D},1} - \Gamma_{1\mathrm{D},2})$, and thus for a small asymmetry in the waveguide decay rate, the coupling to the dark state dominates the dynamics. In addition, we note that the bright state superradiantly decays to the waveguide, and it follows that coupling of probe qubit to the bright state manifest only as contribution of

$$\frac{(2J_{\mathrm{B}})^2}{\Gamma_{1\mathrm{D},1}+\Gamma_{1\mathrm{D},2}} = \Gamma_{1\mathrm{D,p}} \left(\frac{\Gamma_{1\mathrm{D},1}-\Gamma_{1\mathrm{D},2}}{\Gamma_{1\mathrm{D},1}+\Gamma_{1\mathrm{D},2}} \right)^2$$

to the probe qubit decay rate into spurious loss channel. In our experiment, the maximum asymmetry $d = \frac{|\Gamma_{1\mathrm{D},1}-\Gamma_{1\mathrm{D},2}|}{\Gamma_{1\mathrm{D},1}+\Gamma_{1\mathrm{D},2}}$ in waveguide decay rate between qubits is 0.14 (0.03) for type-I (type-II) from Table S-1, and this affects the decay rate of probe qubit by at most $\sim 2\%$.

C. Fitting of Rabi oscillation curves

The Rabi oscillation curves in Fig. 3a and Fig. 4d are modeled using a numerical master equation solver [6, 7]. The qubit parameters used for fitting the Rabi oscillation curves are summarized in Table S-1. For all the qubits, $\Gamma_{1\mathrm{D}}$ was found from spectroscopy. In addition, we have done a time-domain population decay measurement on the probe qubit to find the total decay rate of $\Gamma_1/2\pi = 1.1946$ MHz (95% confidence interval $[1.1644, 1.2263]$ MHz, measured at 6.55 GHz). Using the value of $\Gamma_{1\mathrm{D}}/2\pi = 1.1881$ MHz (95% confidence interval $[1.1550, 1.2211]$ MHz, measured at 6.6 GHz) from spectroscopy, we find the spurious population decay rate $\Gamma_{\mathrm{loss}}/2\pi = \Gamma_1/2\pi - \Gamma_{1\mathrm{D}}/2\pi = 6.5$ kHz (with uncertainty of 45.3 kHz) for the probe qubit. The value of spurious population decay rate is assumed to be identical for all the qubits in the experiment. Note that the decaying rate of the envelope in the Rabi oscillation curve is primarily set by the waveguide decay rate of the probe qubit $\Gamma_{1\mathrm{D,p}}$, and the large relative uncertainty in Γ_{loss} does not substantially affect the fit curve.

The dephasing rate of the probe qubit is derived from time-domain population decay and Ramsey sequence measurements $\Gamma_\varphi = \Gamma_2 - \Gamma_1/2$. In the case of the mirror qubits, the table shows effective single qubit parameters inferred from measurements of the dark state lifetime. We calculate single mirror qubit dephasing rates that theoretically yield the corresponding measured collective value. Assuming an uncorrelated Markovian dephasing for the mirror qubits forming the cavity we find $\Gamma_{\varphi,\mathrm{m}} = \Gamma_{\varphi,\mathrm{D}}$ (See Supplementary Note 3). Similarly, the waveguide decay rate of the mirror qubits is found from the spectroscopy of the bright collective state as $\Gamma_{1\mathrm{D,m}} = \Gamma_{1\mathrm{D,B}}/2$. The detuning between probe qubit and the atomic cavity (Δ) is treated as the only free parameter in our model. The value of Δ sets the visibility and frequency of the Rabi oscillation, and is found from the the fitting algorithm.

Type	Qubits involved	$\Gamma_{1\mathrm{D,p}}/2\pi$ (MHz)	$\Gamma_{1\mathrm{D,m}}/2\pi$ (MHz)	$\Gamma_{\varphi,\mathrm{p}}/2\pi$ (kHz)	$\Gamma_{\varphi,\mathrm{m}}/2\pi$ (kHz)	$\Delta/2\pi$ (MHz)
I	Q_2, Q_6	1.19	13.4	191	210	1.0
II	Q_1, Q_7	0.87	96.7	332	581	5.9
Dark compound	Q_2Q_3, Q_5Q_6	1.19	4.3	191	146	0.9
Bright compound	Q_2Q_3, Q_5Q_6	1.19	20.2	191	253	1.4

TABLE S-1. **Parameters used for fitting Rabi oscillation curves.** The first and second row are the data for 2-qubit dark states, the third and fourth row are the data for 4-qubit dark states made of compound mirrors. Here, $\Gamma_{1\mathrm{D,p}}$ ($\Gamma_{1\mathrm{D,m}}$) is the waveguide decay rate and $\Gamma_{\varphi,\mathrm{p}}$ ($\Gamma_{\varphi,\mathrm{m}}$) is the pure dephasing rate of probe (mirror) qubit, Δ is the detuning between probe qubit and mirror qubits used for fitting the data.

III. SUPPLEMENTARY NOTE 3: LIFETIME (T_1) AND COHERENCE TIME (T_2^*) OF DARK STATE

The dark state of mirror qubits belongs to the decoherence-free subspace in the system due to its collectively suppressed radiation to the waveguide channel. However, there exists non-ideal channels that each qubit is coupled to, and such channels contribute to the finite lifetime (T_1) and coherence time (T_2^*) of the dark state (See Table S-2). In the experiment, we have measured the decoherence rate $\Gamma_{2,\mathrm{D}}$ of the dark state to be always larger than the decay rate $\Gamma_{1,\mathrm{D}}$, which cannot be explained by simple Markovian model of two qubits subject to their own independent noise. We discuss possible scenarios that can give rise to this situation of $\Gamma_{2,\mathrm{D}} > \Gamma_{1,\mathrm{D}}$, with distinction of the Markovian and non-Markovian noise contributions.

There are two major channels that can affect the coherence of the dark state. First, coupling of a qubit to dissipative channels other than the waveguide can give rise to additional decay rate $\Gamma_{\mathrm{loss}} = \Gamma_1 - \Gamma_{1\mathrm{D}}$ (so-called non-radiative decay rate). This type of decoherence is uncorrelated between qubits and is well understood in terms of the Lindblad form of master equation, whose contribution to lifetime and coherence time of dark state is similar as in individual qubit case. Another type of contribution that severely affects the dark state coherence arises from fluctuations in qubit frequency, which manifest as pure dephasing rate Γ_φ in the individual qubit case. This can affect the decoherence of the dark state in two ways: (i) By accumulating a relative phase between different qubit states, this act as a channel to map the dark state into the bright state with short lifetime, and hence contributes to loss of population in the dark state; (ii) fluctuations in qubit frequency also induces the frequency jitter of the dark state and therefore contributes to the dephasing of dark state.

In the following, we model the aforementioned contributions to the decoherence of dark state. Let us consider two qubits separated by $\lambda/2$ along the waveguide on resonance, in the presence of fluctuations $\tilde{\Delta}_j(t)$ in the qubit frequency. The master equation can be written as $\dot{\hat{\rho}} = -i[\hat{H}/\hbar, \hat{\rho}] + \mathcal{L}[\hat{\rho}]$, where the Hamiltonian $\hat{H}$ and the Liouvillian $\mathcal{L}$ are given by

$$\hat{H}(t) = \hbar \sum_{j=1,2} \tilde{\Delta}_j(t) \hat{\sigma}_+^{(j)} \hat{\sigma}_-^{(j)}, \tag{S-22}$$

$$\mathcal{L}[\rho] = \sum_{j,k=1,2} \left[(-1)^{j-k}\Gamma_{1\mathrm{D}} + \delta_{jk}\Gamma_{\mathrm{loss}}\right] \left(\hat{\sigma}_-^{(j)} \hat{\rho} \hat{\sigma}_+^{(k)} - \frac{1}{2}\{\hat{\sigma}_+^{(k)}\hat{\sigma}_-^{(j)}, \hat{\rho}\}\right). \tag{S-23}$$

Here, $\Gamma_{1\mathrm{D}}$ (Γ_{loss}) is the decay rate of qubits into waveguide (spurious loss) channel. Note that we have assumed the magnitude of fluctuation $\tilde{\Delta}_j(t)$ in qubit frequency is small and neglected its effect on exchange interaction and correlated decay. We investigate two scenarios in the following subsections depending on the correlation of noise that gives rise to qubit frequency fluctuations.

A. Markovian noise

If the frequency fluctuations of the individual qubits satisfy the conditions for Born and Markov approximations, i.e. the noise is weakly coupled to the qubit and has short correlation time, the frequency jitter can be described in terms of the standard Lindblad form of dephasing [1].

More generally, we also consider the correlation between frequency jitter of different qubits. Such contribution can arise when different qubits are coupled to a single fluctuating noise source. For instance, if two qubits in a system couple to a magnetic field $B_0 + \tilde{B}(t)$ that is global to the chip with $D_j \equiv \partial\tilde{\Delta}_j/\partial\tilde{B}$, the correlation between detuning of different qubits follows correlation of the fluctuations in magnetic field, giving $\langle\tilde{\Delta}_1(t)\tilde{\Delta}_2(t+\tau)\rangle = D_1 D_2 \langle\tilde{B}(t)\tilde{B}(t+\tau)\rangle \neq 0$.

Type	Qubits involved	$\Gamma_{1,\mathrm{D}}/2\pi$ (kHz)	$\Gamma_{2,\mathrm{D}}/2\pi$ (kHz)
I	Q_2, Q_6	210	366
II	Q_1, Q_7	581	838
Dark compound	Q_2Q_3, Q_5Q_6	146	215
Bright compound	Q_2Q_3, Q_5Q_6	253	376

TABLE S-2. **Decay rate and decoherence rate of dark states.** The first and second row are the data for 2-qubit dark states, the third and fourth row are the data for 4-qubit dark states made of compound mirrors. Here, $\Gamma_{1,\mathrm{D}}$ ($\Gamma_{2,\mathrm{D}}$) is the decay (decoherence) rate of the dark state.

The Liouvillian associated with dephasing can be written as [8]

$$\mathcal{L}_{\varphi,jk}[\hat{\rho}] = \frac{\Gamma_{\varphi,jk}}{2}\left(\hat{\sigma}_z^{(j)}\hat{\rho}\hat{\sigma}_z^{(k)} - \frac{1}{2}\left\{\hat{\sigma}_z^{(k)}\hat{\sigma}_z^{(j)}, \hat{\rho}\right\}\right), \tag{S-24}$$

where the dephasing rate $\Gamma_{\varphi,jk}$ between qubit j and qubit k ($j = k$ denotes individual qubit dephasing and $j \neq k$ is the correlated dephasing) is given by

$$\Gamma_{\varphi,jk} \equiv \frac{1}{2}\int_{-\infty}^{+\infty} \mathrm{d}\tau\, \langle \tilde{\Delta}_j(0)\tilde{\Delta}_k(\tau)\rangle. \tag{S-25}$$

Here, the average $\langle\cdot\rangle$ is taken over an ensemble of fluctuators in the environment. Note that the correlated dephasing rate $\Gamma_{\varphi,jk}$ can be either positive or negative depending on the sign of noise correlation, while the individual pure dephasing rate $\Gamma_{\varphi,jj}$ is always positive.

After we incorporate the frequency jitter as the dephasing contributions to the Liouvillian, the master equation takes the form

$$\dot{\hat{\rho}} = \sum_{j,k=1,2}\left\{\left[(-1)^{j-k}\Gamma_{1\mathrm{D}} + \delta_{jk}\Gamma_{\mathrm{loss}}\right]\left(\hat{\sigma}_-^{(j)}\hat{\rho}\hat{\sigma}_+^{(k)} - \frac{1}{2}\{\hat{\sigma}_+^{(k)}\hat{\sigma}_-^{(j)}, \hat{\rho}\}\right) + \frac{\Gamma_{\varphi,jk}}{2}\left(\hat{\sigma}_z^{(j)}\hat{\rho}\hat{\sigma}_z^{(k)} - \frac{1}{2}\left\{\hat{\sigma}_z^{(k)}\hat{\sigma}_z^{(j)}, \hat{\rho}\right\}\right)\right\}, \tag{S-26}$$

We diagonalize the correlated decay part of the Liouvillian describe the two-qubit system in terms of bright and dark states defined in Eq. (S-15). From now on, we assume the pure dephasing rate and the correlated dephasing rate are identical for the two qubits, and write $\Gamma_\varphi \equiv \Gamma_{\varphi,11} = \Gamma_{\varphi,22}$, $\Gamma_{\varphi,\mathrm{c}} \equiv \Gamma_{\varphi,12} = \Gamma_{\varphi,21}$. For qubits with a large Purcell factor ($\Gamma_{1\mathrm{D}} \gg \Gamma_\varphi, |\Gamma_{\varphi,\mathrm{c}}|, \Gamma_{\mathrm{loss}}$), we can assume that the superradiant states $|\mathrm{B}\rangle$ and $|\mathrm{E}\rangle$ are only virtually populated [9] and neglect the density matrix elements associated with $|\mathrm{B}\rangle$ and $|\mathrm{E}\rangle$. Rewriting Eq. (S-26) in the basis of $\{|\mathrm{G}\rangle, |\mathrm{B}\rangle, |\mathrm{D}\rangle, |\mathrm{E}\rangle\}$, the dynamics related to dark state can be expressed as $\dot{\rho}_{\mathrm{D,D}} \approx -\Gamma_{1,\mathrm{D}}\rho_{\mathrm{D,D}}$ and $\dot{\rho}_{\mathrm{D,G}} \approx -\Gamma_{2,\mathrm{D}}\rho_{\mathrm{D,G}}$, where

$$\Gamma_{1,\mathrm{D}} = \Gamma_{\mathrm{loss}} + \Gamma_\varphi - \Gamma_{\varphi,\mathrm{c}}, \quad \Gamma_{2,\mathrm{D}} = \frac{\Gamma_{\mathrm{loss}}}{2} + \Gamma_\varphi. \tag{S-27}$$

Note that if the correlated dephasing rate $\Gamma_{\varphi,\mathrm{c}}$ is zero, $\Gamma_{1,\mathrm{D}}$ is always larger than $\Gamma_{2,\mathrm{D}}$, which is in contradiction to our measurement result.

We estimate the decay rate into non-ideal channels to be $\Gamma_{\mathrm{loss}}/2\pi = 6.5\,\mathrm{kHz}$ from the difference in Γ_1 and $\Gamma_{1\mathrm{D}}$ of the probe qubit, and assume Γ_{loss} to be similar for all the qubits. Applying Eq. (S-27) to measured values of $\Gamma_{2,\mathrm{D}}$ listed in Table S-2, we expect that the pure dephasing of the individual qubit is the dominant decay and decoherence source for the dark state. In addition, we compare the decay rate $\Gamma_{1,\mathrm{D}}$ and decoherence rate $\Gamma_{2,\mathrm{D}}$ of dark states in the Markovian noise model and infer that the correlated dephasing rate $\Gamma_{\varphi,\mathrm{c}}$ is positive and is around a third of the individual dephasing rate Γ_φ for all types of mirror qubits.

B. Non-Markovian noise

In a realistic experimental setup, there also exists non-Markovian noise sources contributing to the dephasing of the qubits, e.g. $1/f$-noise or quasi-static noise [10–12]. In such cases, the frequency jitter cannot be simply put into the Lindblad form as described above. In this subsection, we consider how the individual qubit dephasing induced by non-Markovian noise influences the decoherence of dark state. As shown below, we find that a non-Markovian noise source can lead to a shorter coherence time to lifetime ratio for the dark states, in a similar fashion to correlated dephasing. However, we find that the functional form of the visibility of Ramsey fringes is not necessarily an exponential for a non-Markovian noise source.

We start from the master equation introduced in Eqs. (S-22)-(S-23) can be written in terms of the basis of $\{|\mathrm{G}\rangle, |\mathrm{B}\rangle, |\mathrm{D}\rangle, |\mathrm{E}\rangle\}$,

$$\dot{\hat{\rho}} = -\frac{i}{\hbar}[\hat{H}, \hat{\rho}] + (2\Gamma_{1\mathrm{D}} + \Gamma_{\mathrm{loss}})\,\mathcal{D}[\hat{S}_{\mathrm{B}}]\hat{\rho} + \Gamma_{\mathrm{loss}}\mathcal{D}[\hat{S}_{\mathrm{D}}]\hat{\rho}, \tag{S-28}$$

where the Hamiltonian is written using the common frequency jitter $\tilde{\Delta}_c(t) \equiv [\tilde{\Delta}_1(t) + \tilde{\Delta}_2(t)]/2$ and differential frequency jitter $\tilde{\Delta}_d(t) \equiv [\tilde{\Delta}_1(t) - \tilde{\Delta}_2(t)]/2$

$$\hat{H}(t)/\hbar = \tilde{\Delta}_c(t)\,(2|\mathrm{E}\rangle\langle\mathrm{E}| + |\mathrm{D}\rangle\langle\mathrm{D}| + |\mathrm{B}\rangle\langle\mathrm{B}|) + \tilde{\Delta}_d(t)\,(|\mathrm{B}\rangle\langle\mathrm{D}| + |\mathrm{D}\rangle\langle\mathrm{B}|)\,. \tag{S-29}$$

Here, $\hat{S}_{\mathrm{B}}$ and $\hat{S}_{\mathrm{D}}$ are defined in Eq. (S-16). From the Hamiltonian in Eq. (S-29), we see that the common part of frequency fluctuation $\tilde{\Delta}_c(t)$ results in the frequency jitter of the dark state while the differential part of frequency fluctuation $\tilde{\Delta}_d(t)$ drives the transition between $|\mathrm{D}\rangle$ and $|\mathrm{B}\rangle$, which acts as a decay channel for the dark state.

For uncorrelated low-frequency noise on the two qubits, the decoherence rate is approximately the standard deviation of the common frequency jitter $\sqrt{\langle\tilde{\Delta}_c(t)^2\rangle}$. The decay rate in this model can be found by modeling the bright state as a cavity in the Purcell regime, and calculate the damping rate of the dark state using the Purcell factor as $\langle 4\tilde{\Delta}_d(t)^2/\Gamma_{\mathrm{B}}\rangle$. As evident, in this model the dark state's population decay rate is strongly suppressed by the large damping rate of bright state Γ_{B}, while the dark state's coherence time can be sharply reduced due to dephasing.

IV. SUPPLEMENTARY NOTE 4: SHELVING

We consider the case of two identical mirror qubits of frequency $\omega_{\rm q}$, separated by distance $\lambda/2$ along the waveguide. In addition to free evolution of qubits, we include a coherent probe signal from the waveguide in the analysis. In the absence of pure dephasing ($\Gamma_\varphi = 0$) and thermal occupancy ($\bar{n}_{\rm th} = 0$), the master equation in the rotating frame of the probe signal takes the same form as Eq. (S-28), where the Hamiltonian containing the drive from the probe signal is written as

$$\hat{H}/\hbar = \sum_{\mu={\rm B,D}} \left[-\delta\omega\ \hat{S}_\mu^\dagger \hat{S}_\mu + \frac{\Omega_\mu}{2}\left(\hat{S}_\mu + \hat{S}_\mu^\dagger\right)\right], \tag{S-30}$$

where $\hat{S}_{\rm B}$ and $\hat{S}_{\rm D}$ are defined in Eq. (S-16), $\delta\omega = \omega_{\rm p} - \omega_{\rm q}$ is the detuning of the probe signal from the mirror qubit frequency, Ω_μ is the corresponding driven Rabi frequency. Note that due to the symmetry of the excitations with respect to the waveguide, we see that $\Omega_{\rm D} = 0$ and $\Omega_{\rm B} = \sqrt{2}\Omega_1$, where Ω_1 is the Rabi frequency of one of the mirror qubits from the probe signal along the waveguide.

Let us consider the limit where the Purcell factor $P_{\rm 1D} = \Gamma_{\rm 1D}/\Gamma'$ of qubits is much larger than unity (equivalent to $\Gamma_{\rm D} = \Gamma' \ll \Gamma_{\rm B} = 2\Gamma_{\rm 1D} + \Gamma'$) and the drive applied to the qubits is weak $\Omega_{\rm B} \ll \Gamma_{\rm B}$. Then, we can effectively remove some of the density matrix elements [13],

$$\rho_{\rm E,E},\ \rho_{\rm B,E},\ \rho_{\rm E,B},\ \rho_{\rm G,E},\ \rho_{\rm E,G} \approx 0$$

and restrict the analysis to ones involved with three levels $\{|{\rm G}\rangle, |{\rm D}\rangle, |{\rm B}\rangle\}$. In addition, the dark state $|{\rm D}\rangle$ is effectively decoupled from $|{\rm G}\rangle$ and $|{\rm B}\rangle$, acting as a metastable state. Therefore, we only consider the following set of the master equation:

$$\dot{\rho}_{\rm B,B} \approx -\Gamma_{\rm B}\,\rho_{\rm B,B} + \frac{i\Omega_{\rm B}}{2}(\rho_{\rm B,G} - \rho_{\rm G,B}) \tag{S-31}$$

$$\dot{\rho}_{\rm B,G} \approx \left(i\delta\omega - \frac{\Gamma_{\rm B}}{2}\right)\rho_{\rm B,G} + \frac{i\Omega_{\rm B}}{2}(\rho_{\rm B,B} - \rho_{\rm G,G}) \tag{S-32}$$

$$\dot{\rho}_{\rm G,G} \approx -\dot{\rho}_{\rm B,B}; \quad \dot{\rho}_{\rm G,B} = \dot{\rho}_{\rm B,G}^* \tag{S-33}$$

Using the normalization of total population $\rho_{\rm G,G} + \rho_{\rm D,D} + \rho_{\rm B,B} \approx 1$ with Eqs. (S-31)-(S-33), we obtain the approximate steady-state solution

$$\langle \hat{S}_{\rm B} \rangle \approx \rho_{\rm B,G} \approx -\frac{i\Omega_{\rm B}(1-\rho_{\rm D,D})}{\Gamma_{\rm B} - 2i\delta\omega}. \tag{S-34}$$

The input-output relation [2] is given as

$$\hat{a}_{\rm out} = \hat{a}_{\rm in} + \sqrt{\frac{\Gamma_{\rm 1D}}{2}}\hat{\sigma}_-^{(1)} - \sqrt{\frac{\Gamma_{\rm 1D}}{2}}\hat{\sigma}_-^{(2)} = \hat{a}_{\rm in} + \sqrt{\Gamma_{\rm 1D}}\hat{S}_{\rm B}, \tag{S-35}$$

where $\hat{a}_{\rm in}$ is the input field operator and $\hat{a}_{\rm out}$ is the operator for output field propagating in the same direction as the input field (here, the input field is assumed to be incident from only one direction). The transmission amplitude is calculated as

$$t = \frac{\langle \hat{a}_{\rm out}\rangle}{\langle \hat{a}_{\rm in}\rangle} = 1 - \frac{(1-\rho_{\rm D,D})\Gamma_{\rm 1D}}{-i\delta\omega + \Gamma_{\rm B}/2} \tag{S-36}$$

where the relation $\Omega_1/2 = -i\langle \hat{a}_{\rm in}\rangle\sqrt{\Gamma_{\rm 1D}/2}$ has been used.

In the measurement, we use the state transfer protocol to transfer part of the ground state population into the dark state. Following this, we drive the $|{\rm G}\rangle \leftrightarrow |{\rm B}\rangle$ transition by sending a weak coherent pulse with a duration 260 ns into the waveguide, and recording the transmission spectrum. As a comparison, we also measure the transmission spectrum when the mirror qubits are in the ground state, which corresponds to having $\rho_{\rm D,D} = 0$. The transmittance in the two cases (Figure 3d) are fitted with identical parameters for $\Gamma_{\rm 1D}$ and $\Gamma_{\rm B}$. The dark state population $\rho_{\rm D,D}$ following the iSWAP gate is extracted from the data as 0.58, which is lower than the value (0.68) found from the Rabi oscillation peaks (Figure 3a). The lower value of the dark state population can be understood considering the finite lifetime of dark state (757 ns), which leads to a partial population decay during the measurement time (the single-shot measurement time is set by the duration of the input pulse). It should be noted that the input pulse has a transform-limited bandwidth of ~ 3.8 MHz, which results in frequency averaging of the spectral response over this bandwidth. For this reason, the on-resonance transmission extinction measured in the pulsed scheme is lower than the value found from continuous wave (CW) measurement (Figure 1c).

[1] C. Gardiner and P. Zoller, *Quantum Noise* (Springer, 2004).
[2] K. Lalumière, B. C. Sanders, A. F. van Loo, A. Fedorov, A. Wallraff, and A. Blais, Phys. Rev. A **88**, 043806 (2013).
[3] O. Astafiev, A. M. Zagoskin, A. A. Abdumalikov, Y. A. Pashkin, T. Yamamoto, K. Inomata, Y. Nakamura, and J. S. Tsai, Science **327**, 840 (2010).
[4] B. Peropadre, J. Lindkvist, I.-C. Hoi, C. M. Wilson, J. J. Garcia-Ripoll, P. Delsing, and G. Johansson, New J. Phys. **15**, 035009 (2013).
[5] J.-H. Yeh, J. LeFebvre, S. Premaratne, F. C. Wellstood, and B. S. Palmer, J. Appl. Phys. **121**, 224501 (2017).
[6] J. Johansson, P. Nation, and F. Nori, Comput. Phys. Commun. **183**, 1760 (2012).
[7] J. Johansson, P. Nation, and F. Nori, Comput. Phys. Commun. **184**, 1234 (2013).
[8] L.-M. Duan and G.-C. Guo, arXiv:quant-ph/9811058 (1998).
[9] V. Paulisch, H. J. Kimble, and A. González-Tudela, New J. Phys. **18**, 043041 (2016).
[10] J. M. Martinis, S. Nam, J. Aumentado, K. Lang, and C. Urbina, Phys. Rev. B **67**, 094510 (2003).
[11] G. Ithier, E. Collin, P. Joyez, P. J. Meeson, D. Vion, D. Esteve, F. Chiarello, A. Shnirman, Y. Makhlin, J. Schriefl, and G. Schön, Phys. Rev. B **72**, 134519 (2005).
[12] J. Koch, M. Y. Terri, J. Gambetta, A. A. Houck, D. Schuster, J. Majer, A. Blais, M. H. Devoret, S. M. Girvin, and R. J. Schoelkopf, Phys. Rev. A **76**, 042319 (2007).

[13] From the master equation, the time-evolution of part of the density matrix elements are approximately written as

$$
\begin{aligned}
\dot{\rho}_{\mathrm{E,E}} &= -(\Gamma_{\mathrm{B}}+\Gamma_{\mathrm{D}})\rho_{\mathrm{E,E}} + \frac{i\Omega_{\mathrm{B}}}{2}(\rho_{\mathrm{B,E}}-\rho_{\mathrm{E,B}}),\\
\dot{\rho}_{\mathrm{E,B}} &= \left[i\delta\omega - \left(\Gamma_{\mathrm{B}}+\frac{\Gamma_{\mathrm{D}}}{2}\right)\right]\rho_{\mathrm{E,B}} + \frac{i\Omega_{\mathrm{B}}}{2}(\rho_{\mathrm{B,B}}-\rho_{\mathrm{E,E}}+\rho_{\mathrm{E,G}}),\\
\dot{\rho}_{\mathrm{E,G}} &= \left(2i\delta\omega - \frac{\Gamma_{\mathrm{B}}+\Gamma_{\mathrm{D}}}{2}\right)\rho_{\mathrm{E,G}} + \frac{i\Omega_{\mathrm{B}}}{2}(\rho_{\mathrm{B,G}}+\rho_{\mathrm{E,B}}),\\
\dot{\rho}_{\mathrm{E,B}} &= \dot{\rho}^{*}_{\mathrm{B,E}}; \quad \dot{\rho}_{\mathrm{E,G}} = \dot{\rho}^{*}_{\mathrm{G,E}}.
\end{aligned}
$$

In the steady state, it can be shown that

$$
\begin{aligned}
\rho_{\mathrm{E,E}} &\sim \mathcal{O}(x^2)\rho_{\mathrm{B,B}} + \mathcal{O}(x^3)(\rho_{\mathrm{B,G}}-\rho_{\mathrm{G,B}})\\
\rho_{\mathrm{B,E}} &\sim \mathcal{O}(x)\rho_{\mathrm{B,B}} + \mathcal{O}(x^2)\rho_{\mathrm{G,B}}\\
\rho_{\mathrm{G,E}} &\sim \mathcal{O}(x^2)\rho_{\mathrm{B,B}} + \mathcal{O}(x)\rho_{\mathrm{G,B}}
\end{aligned}
$$

to leading order in $x \equiv \Omega_{\mathrm{B}}/\Gamma_{\mathrm{B}} < 1$, and hence we can neglect the contributions from $\rho_{\mathrm{E,E}}$, $\rho_{\mathrm{B,E}}$, $\rho_{\mathrm{E,B}}$, $\rho_{\mathrm{G,E}}$, $\rho_{\mathrm{E,G}}$ from the analysis in the weak driving limit. The probe power we have used in the experiment corresponds to $x \sim 0.15$, which makes this approximation valid.